

# PREDIS

## WP.7 Task 7.2.2

### Reference package and factors affecting package evolution and degradation

31/08/2021 version 2.0

Dissemination level: Public

**Alex Potts**

National Nuclear Laboratory  
Workington Laboratory, Havelock Road, Cumbria, U.K.

[alexander.potts@uknnl.com](mailto:alexander.potts@uknnl.com)  
01900 513370



Project acronym PREDIS	Project title PRE-DISposal management of radioactive waste	Grant agreement No. 945098
Deliverable No. D7.2.2	Deliverable title Reference package and factors affecting package evolution and degradation	Version 2.0
Type Technical Memorandum	Dissemination level Public	Due date 31/08/21
Lead beneficiary		WP No. 7.2
Main author Alex Potts (NNL)	Reviewed by Steve Palethorpe (NNL)	Accepted by Martin Hayes (NNL)
Contributing author(s) Darren Potter		Pages 26

#### Abstract

The European project for pre-disposal management of radioactive waste (PREDIS) consists of several work packages (WPs), including WP 7 “Innovations in cemented waste handling and pre-disposal storage”. This document includes a table of end user waste packages, which was sourced using data from the PREDIS WP7.1 state of the art (SoTA) report and Nuclear Decommissioning Authority (NDA) reports.

The collected data was used to provide a cemented waste package to be used as a point of reference throughout the rest of WP7. For the reference package, details such as geometry, grout matrix and waste container material are provided. Reactive metals, in particular Magnox or magnesium metal, are presented as a reference degradation mechanism which should be used to cause the degradation of the grout matrix and package. Additionally, several key areas where variants may want to be investigated are included, such as the use of aluminium metal instead of Magnox to generate corrosion.

#### Coordinator contact

Maria Oksa  
VTT Technical Research Centre of Finland Ltd  
Kivimiehentie 3, Espoo / P.O. Box 1000, 02044 VTT, Finland  
E-mail: [maria.oksa@vtt.fi](mailto:maria.oksa@vtt.fi)  
Tel: +358 50 5365 844

#### Notification

The use of the name of any authors or organization in advertising or publication in part of this report is only permissible with written authorisation from the VTT Technical Research Centre of Finland Ltd.

#### Acknowledgement

This project has received funding from the Euratom research and training programme 2019-2020 under grant agreement No 945098.

## HISTORY OF CHANGES

Date	Version	Author	Comments
01/07/2021	0	Alex Potts	Issued as draft
02/08/2021	1.0	Alex Potts	Issue 1.0 addressing comments from the draft
31/08/2021	2.0	Alex Potts	Issue 2.0 addressing minor comments from the first issue

## TABLE OF CONTENTS

1	INTRODUCTION.....	5
2	BACKGROUND.....	5
2.1	Packages.....	5
2.2	Degradation Mechanisms.....	5
2.2.1	Carbonation.....	5
2.2.2	Alkali aggregate reaction (AAR).....	6
2.2.3	Radiation damage.....	6
2.2.4	Metal corrosion.....	7
2.2.5	Chloride Corrosion.....	8
2.2.6	Chemical reactions.....	9
2.2.7	Organic Material Degradation.....	9
2.3	Reference Degradation Mechanism.....	11
3	REFERENCE PACKAGE.....	13
3.1	Waste package geometry and construction.....	13
3.2	Other details for reference package.....	15
4	CONCLUSIONS.....	15
5	OPTIONAL VARIANTS.....	16

## 1 Introduction

The European project for pre-disposal management of radioactive waste (PREDIS) consists of several work packages (WPs), including WP 7 “Innovations in cemented waste handling and pre-disposal storage” [1]. This WP is broken down into several sub WPs, which aim to address a variety of challenges, such as:

- Identifying monitoring technologies,
- Develop digital twin technology,
- Identifying opportunities for increased store automation,
- Identify chemical and mineralogical package evolution mechanisms.

## 2 Background

### 2.1 Packages

As part of the State of the Art (SoTA) report undertaken for WP7.1 [1], PREDIS partners provided information on the various waste packages relevant to their home countries. This information was collated into a spreadsheet, included with this technical memorandum, and used to highlight different trends within the data. Further waste packages relevant to the U.K. were also added to the spreadsheet based on the guidance and specification for 6 m<sup>3</sup> boxes [2] and 500 L drums [3]. A summary of this spreadsheet can be found in the Appendices in Table 4.

### 2.2 Degradation Mechanisms

A detailed review on the durability of concrete for low level waste (LLW) and high level waste (HLW) can be found in reference [4] as well as in the SoTA report itself [1]. In the latter report, six out of eight responders detailed that the following degradation mechanisms had been indicated as of interest/ observed:

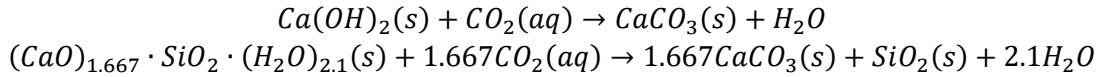
- Internal/ external corrosion,
- Cracks linked to the handling of the package,
- Alkali-silica reaction (ASR) gel formation,
- Leakage of Liquids
- Swelling
- Chemical reactions.

Given the significant body of work that exists, this document will only provide a high-level overview of the above. Leakage of liquids and swelling will not be discussed as they can be thought of as consequences of wasteform evolution rather than degradation mechanisms in themselves, even though those two processes may cause damage to a container. Instead the focus will be on the processes that lead to either wasteform (and potentially waste container) swelling or loss of waste containment e.g. leaking liquid. Similarly, cracking linked to the handling of the packages is not discussed. Although not listed above carbonation is also briefly discussed as a long-term atmospheric process that can affect the wasteform for both stainless steel and concrete containers and the container itself, if it is of concrete construction. Similarly, radiation damage is also discussed due to it being both an internal mechanism (from the waste itself) and an external process (irradiation by surrounding packages). Each mechanism is discussed briefly below:

#### 2.2.1 Carbonation

Carbonation is a reaction that occurs between carbon dioxide (usually but not always from the atmosphere) and the Ca containing phases present within the hydrated cement microstructure,

namely calcium hydroxide (Ca(OH)<sub>2</sub>) and calcium-silicate-hydrate (C-S-H) to form calcium carbonate [1]. The carbonation process can be broken down into three main steps: the dissolution of the calcium containing phases into the pore water, adsorption of carbonate ions produced from dissolved CO<sub>2</sub> in the cement pore solution, followed by the precipitation of calcium carbonate [5], with the overall chemical reaction [1] detailed in Equation 1, involving the simultaneous dissolution of Ca(OH)<sub>2</sub> and the decalcification of the C-S-H phase.



*Equation 1: Carbonation reaction equations*

Carbon dioxide consumes OH<sup>-</sup> ions in the pore water to form the carbonate species which subsequently react with Ca<sup>2+</sup> ions, resulting in the precipitation of calcium carbonate, and leading to a decrease in the pore water pH of a cement matrix from 12.5+ to 8-10, at which point the passivation provided to any steel in the cementitious mass by the high alkalinity is lost and the steel will corrode [5]–[8]. This is a common issue with reinforcement steel leading to cracking and spalling of cover material from reinforced concrete. This may affect concrete radwaste containers if adequate reinforcement cover is not in place and appropriate storage environment is not maintained. The formation of calcium carbonate is also associated with a volumetric expansion [5], which can result in cement cracking and a reduction in the pore volume. However, work investigating cement based nuclear wasteforms at 500 L drum scale found a maximum carbonation ingress of 3 mm despite the samples being ~10 years old and stored in uncontrolled normal atmospheric conditions [9]. This shows that carbonation is unlikely to be a significant issue for cemented nuclear waste.

### 2.2.2 Alkali aggregate reaction (AAR)

Alkali aggregate reaction (AAR) typically refers to the deleterious reaction between certain forms of silica present in concrete aggregates and the alkaline pore water present in a cement medium, giving rise to an alkali silica reaction (ASR) [1], [4], [10]. There is also a form of the reaction that occurs between carbonate and alkaline pore water referred to as the alkali carbonate reaction (ACR) [10]. These AAR's form a gel that absorb water and volumetrically expand, resulting in cracking of the concrete. These reactions normally occur when the silica or carbonate are provided via aggregate, making them unlikely to occur in the nuclear wasteform which typically uses grouts rather than concrete. It could however occur in concrete used for the waste package construction such as a concrete box or concrete layer in double skinned drums. It may also be possible for an AAR type reaction to occur if the reactive silica/ carbonate normally present in the aggregate were to be present in the nuclear waste itself. This idea has some substantiation as there have been reports of ASR occurring within cemented waste packages [11], however it is unclear if this is referring to the typical ASR reaction associated with aggregate.

### 2.2.3 Radiation damage

Radiation damage of cement and concretes has been examined by several papers. For gamma radiation, the literature has noted the following effects: changes in the porosity [12], [13], reductions in compressive strength [12]–[14] and increased carbonation ingress [15]. Gamma radiation also contributes to hydrogen gas generation through radiolysis of both the pore water and gel water [16] in addition to the breakdown of organic waste components [17], which can lead to package pressurisation and potentially swelling. It is noted that in the U.K. there has been a significant body of work to show that radiolytic hydrogen gas generation can be effectively managed using suitably developed permeable grout matrices and vented packages [18], [19]. The effects of the neutron irradiation literature are not discussed due to it being more applicable to nuclear power plants. Whilst alpha radiation studies on grouted wasteforms are applicable, there has only been a limited amount

of research carried out at present due to the high costs of experimentation, requiring the immobilization of an alpha-emitter to realistically assess the internal pressurization effects on wasteforms as a result of the short penetrating range of alpha radiation causing radiolysis of the aqueous phase in regions of closed or low porosity within the matrix [20].

#### 2.2.4 Metal corrosion

Metal corrosion was also identified as a potential degradation mechanism within the SoTA report [1], that affects both the waste container itself as well as the metal encapsulated in the wasteform which can subsequently impact on the waste container. In a cemented waste form, this can occur due to the incorporated waste itself, with aluminum, Magnox and uranium all being examples of reactive metals cited in the literature [4]. These metals can corrode in both aerobic and anaerobic alkaline conditions, such as those found in a cemented nuclear waste package [4]. The corrosion products formed occupy a greater volume than the parent metal, which results in cement cracking even at as little corrosion as 0.014-0.016 % [21]. As the metal continues to corrode the induced stress in the grout wasteform continues to increase [22]. It is noted that whilst reactive metals corrosion in nuclear waste treatment processes is typically thought of in terms of aluminum, Magnox and uranium corrosion, steel also poses a long-term issue given the large volumes present in decommissioning wastes, as it will also corrode over long timescales, forming a similarly expansive product.

In a Magnox system, there is an initial stage after grouting, in which the corrosion rate is greater, called acute corrosion, which then transitions into a steadier long-term chronic corrosion rate [4]. It has been shown in grout that Magnox also goes through a transitional intermediate phase, before reaching the long-term steady state chronic rate which may take several months/years [4]. In the case of Magnox corrosion in grout matrices, the chronic corrosion rate increases with temperature [23] and also increases when subsequently exposed to chloride after immobilization e.g. if the wasteform is cracked and exposed to chloride under saturated long-term repository conditions [4]. Conversely, if chloride is present in the grout mix water, an increase in the corrosion rate is notable only at concentrations greater than 2000 ppm [4]. The corrosion reactions can lead to the generation of hydrogen gas, which has the same effects as hydrogen generation due to radiolysis. An example reaction is given for Magnox [24].



*Equation 2: Magnox corrosion reaction*

For Magnox, the long-term chronic corrosion rate in grout at 298 K is  $\sim 0.2 \mu\text{m}\cdot\text{a}^{-1}$  [25], whereas mild steel possesses a chronic corrosion rate under anaerobic conditions (anticipated in a cemented wasteform containing a blast furnace slag component) of  $\sim 0.01 \mu\text{m}\cdot\text{a}^{-1}$ , which shows little temperature dependence [26]. The corresponding volumetric expansion can also be calculated by accounting for the difference in density of the corrosion products formed. Table 1 provides an illustrative comparison of calculated volumetric expansion amounts for mild steel, Magnox and aluminium in grout media, which were taken from reference [4]. The values included were selected from typical storage conditions calculations, which made the following assumptions:

- Surface storage at 20 °C for 100 years,
- GDF operational phase temperature of 30 °C for 150 years,
- Backfilling and post-closure temperature of 50 °C up to 1000 years,
- Steel and aluminium were assumed to be in the form of sheet geometries (500 mm x 500 mm x 6 mm),
- Maghaemite was assumed to be the corrosion product formed from iron corrosion, as this would yield the largest volumetric expansion of possible corrosion products formed.
- Magnox was in the form of swarf of surface area  $1.39 \text{ m}^2/\text{kg}$

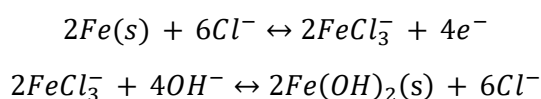
Table 1: Calculated volumetric expansion values in grout media for mild steel, Magnox and aluminium in surface store conditions at 20 °C. Taken from reference [4].

Time (years)	Volume expansion (L/kg of original metal)		
	Mild Steel	Magnox	Aluminium
100	0.0001	0.058	0.088
250	0.0003	0.275	0.088
1000	0.0010	1.260	0.088

The figures in Table 1 show that Magnox corrosion under the conditions assumed results in a significantly greater amount of volumetric expansion in grouted wastefoms than both mild steel and aluminium over 1000 years. Aluminium is an interesting case as it appears to offer a greater volumetric expansion than Magnox over short timescales making it ideal as a degradation simulator. However, aluminium possesses a very high acute corrosion rate followed by a rapid decrease to negligible levels, which occurs within the first 24 hours of the grout contacting the aluminium surface [4]. This trend of rapid corrosion (on the order of  $10^2$  -  $10^3$   $\mu\text{m}\cdot\text{a}^{-1}$ ) followed by a sharp decrease in corrosion rate has been observed by several papers [27]–[29]. This means that the peak corrosion rate occurs whilst the cement is in a plastic state, with the associated hydrogen generation creating voidage in the cement at the grout/metal interface; this voidage can then accommodate the volumetric expansion from the corrosion products meaning that aluminium corrosion is not anticipated to significantly alter the performance of the bulk wasteform or the container [30]. This porous phase surrounding the aluminium has also been reported in other studies [29], [31], with Setiadi et al., reporting microcracking of the cement at  $\approx$  90 days for OPC cements and  $\approx$  720 days for a blast furnace slag (BFS) blended system [29]. It has also been reported that aluminium corrosion can persist in higher pH grout systems i.e. those containing only CEM I powder, however, these results were observed only when the grout sample was re-saturated with alkaline water by immersion in solution to restart corrosion, which is not representative of normal storage conditions (but could be applicable in the case of a repository flooding) [27]. When exposed to increased humidity atmospheres (>95 % RH), the corrosion did restart for a CEM I only grout formulation, however, it was at a significantly reduced level ( $0.45$   $\mu\text{m}\cdot\text{a}^{-1}$  after 1 year exposure) compared to the alkaline water re-saturation (several hundred  $\mu\text{m}\cdot\text{a}^{-1}$  after  $\sim$ 4 months exposure). It is noteworthy that this trend only occurred in the CEM I system, whereas a high BFS replacement CEM III/C grout did not show a corrosion restart even after 1200 hours of re-saturation in the alkaline water or when subjected to high relative humidity environments. This comparison of OPC cement systems being more affected by aluminium corrosion than BFS blended cements is also in line with the literature [29], [32].

### 2.2.5 Chloride Corrosion

Corrosion can also occur due to chloride interaction, which can occur due to exposure to external chloride conditions or from chloride content in the concrete/cement matrix itself [1]. In this scenario chloride ions do not partake in the corrosion reaction but break down the passivating layer that protects the steel, accelerating corrosion. The chloride ions also interact with iron to form  $\text{FeCl}_3^-$  which is unstable and leads to the formation of the expansive  $\text{Fe}(\text{OH})_2$  product [4]. This reaction scheme is detailed in Equation 3.



Equation 3: Chloride corrosion reaction scheme

## 2.2.6 Chemical reactions

The final degradation mechanism listed as of interest in the SoTA report is from chemical reactions, which in this report is discussed as sulfate attack. In the case of sulfate attack, dissolved  $SO_4^{2-}$  can react with calcium hydroxide to form gypsum, which is an expansive reaction [4]. The newly formed gypsum can then react with further sulfate ions, to form ettringite (calcium sulpho-aluminate,  $C_6AS_3H_{32}$ ), which is a highly expansive phase and so can lead to cracking of the cement phase. Ettringite can also be formed directly from the reaction of monosulfate ( $C_4ASH_{12}$ ) with Ca in a sulfate rich environment. If metastable monosulfate is formed, a delayed ettringite formation (DEF) reaction can subsequently occur, where ettringite is formed at later ages in curing and can lead to the cement matrix cracking due to volumetric expansion [33], [34]. At high hydration temperatures ( $>70$  °C) [4], [34] ettringite can decompose into monosulfate which could subsequently result in DEF if temperatures are lowered in a Ca and sulfate rich environment.

## 2.2.7 Organic Material Degradation

Whilst not specifically singled out in the SoTA report [1] by the respondents, degradation of organic material can lead to package degradation and so a small summary is included here. Microbial degradation specifically refers to the biochemical processes caused by the activity of micro-organisms which can impact the durability of cement and concrete. Examples of micro-organisms that may be present are *thiobacillus thiooxidans* and *thiobacillus ferrooxidans*, which are sulphur-oxidising bacteria [4]. In the presence of sulphur, these bacteria will produce sulphuric acid, increasing the probability of sulfate attack; this is more likely to occur in a BFS system due to the sulfide content (typically 1-4 wt%) associated with the BFS itself [35]. However, these bacteria are most efficient in aerobic conditions and at a pH range of 2 - 4.5. The significantly higher pH range of Portland cement based wasteforms means sustained microbial attack is unlikely [4].

Organic material degradation can also occur through organic waste, e.g. cellulose containing material, being encapsulated [1]. Organic materials can be separated into two categories: slowly decomposable and rapidly decomposable [36], with cellulose being taken as an important example of the latter category. There are several scenarios under which a gaseous product can be formed from cellulose degradation [1], which will lead to similar consequences to gas production from radiolysis in terms of package pressurization. Carbon dioxide will be formed when the pH is  $\sim 11$  in oxidising or anaerobic conditions, whereas strongly reducing conditions will lead to  $CO_2$  and  $CH_4$  gas being produced. In a recent paper, where cellulose was encapsulated with plutonium in blended Portland cement grouts, the addition of cellulose substantially increased the radiolytic hydrogen yield [17]. There have been several other papers examining the effects of cellulose degradation, however, these have used synthesised cement pore solutions [37]–[39].

A summary table of the aforementioned degradation mechanisms is provided in Table 2, which describes the mechanism, what changes may result, and the consequences of this change on the wasteform/package. Cement cracking will lead to a reduction in waste immobilisation integrity as well as provide greater opportunity for ingress by air or other species (e.g. chloride) which could cause further degradation reactions. Volumetric expansion will cause cracking of the cement phase but can also lead to package deformation if the expansion is sufficient, which can lead to an initial loss of package stacking stability, affecting the ability to handle the packages and make marking illegible, and ultimately, if distortion is large enough may lead to loss of container integrity. Waste package pressurisation due to hydrogen production could have potentially similar effects to that of volumetric expansion in terms of package deformation in the case of sealed packages, but also creates a potentially explosive gas pocket if not managed.

Table 2: Summary of the different degradation mechanisms, their resulting changes to the wasteform and package.

Degradation Mechanism	What is caused	Effect on the package/wasteform	Comment
Carbonation	Drop in grout pH, expansive carbonate phases formed	Drop in pH can reduce passivation of metals and allow for metallic corrosion, i.e. if carbon steel package is used. Cement cracking due to carbonate formation.	Only occurs to small extent. The reduction in porosity could potentially be a positive.
ASR	Expansive reaction with a gel like layer formed	Grout cracking, wasteform expansion.	Should be minimal in grout matrix due to lack of aggregate. Evidence silica present in nuclear waste could contribute however.
Reactive Metal Corrosion	Expansion, H <sub>2</sub> gas production	Wasteform cracking and package deformation/ perforation due to expansion. Waste package pressurisation from H <sub>2</sub> gas generation if not managed.	Typically associated with aluminium, Magnox and uranium from the nuclear waste. Steel could also be an issue as it will corrode given enough time and forms similarly expansive products as the other metals mentioned. Main method of controlling the reaction is via limiting amount of reactive metal in the packages.
Chloride Corrosion	Expansion Deterioration of container	Wasteform cracking and package deformation due to expansion. General and pitting corrosion of container - may result in breach of containment and/or loss of strength.	Can be managed internally by controlling chloride content in the cement powder. Canister deterioration can be managed externally by wearing gloves and managing chloride content in atmosphere.

Degradation Mechanism	What is caused	Effect on the package/wasteform	Comment
Chemical Processes	Expansion	Wasteform cracking and package deformation due to expansion.	Can be managed by controlling sulfate content and using grout formulations with low heat exotherms.
Radiolysis/Radiation Damage	H <sub>2</sub> gas production	Waste package pressurisation from H <sub>2</sub> gas generation if not managed.	Can be managed through grout formulation and vented packages.
Organic Decomposition	Multiple mechanisms depending on the waste (e.g. gas production, sulfate attack etc.)	Wasteform cracking and package deformation due to expansion. Waste package pressurisation from H <sub>2</sub> gas generation if not managed.	There are numerous ways in which this mechanism can occur, each which can cause different effects. High pH formulations should reduce microbial degradation. Controlling organic material loading into cement will reduce this mechanism.

## 2.3 Reference Degradation Mechanism

One clear trend from the degradation mechanisms listed as of interest by the PREDIS partners is that the most common degradation ‘consequence’ is volumetric expansion, which will lead to cracking of the cement matrix and potentially package deformation. Given only a small amount of corrosion is required before surface cracking occurs, for example between 0.1 % and 1.7 % corrosion for steel<sup>1</sup> in a cement matrix [21], combined with the fact that the internal stresses only increase with corrosion amount [22], reactive metal corrosion will likely be a significant contributor to wasteform degradation. Therefore, the reference degradation mechanism should be to examine wasteform cracking and package deformation due to corrosion of reactive metals. There are two cases that can be assessed for this:

1. local corrosion and expansion due to a singular large metal piece,
2. global expansion due to small pieces of metal dispersed homogeneously within the grout matrix.

It is recommended that Magnox metal be used to generate corrosion, however, Mg metal can also be used as a substitute. Whilst uranium offers better applicability to the wider PREDIS partners, the active nature of the material may make it impractical to use in experimental trials. Aluminum was also considered, however, the acute corrosion rate, whilst high (typically  $\sim 15,000 \mu\text{m}\cdot\text{a}^{-1}$ ) is very short lived (0.365 days) [26], which is followed by a chronic corrosion rate that ultimately decreases linearly to negligible levels with time meaning actual expansion of the waste package is unlikely [27], [30]. Steel was also considered as a reference reactive metal as it is applicable for multiple PREDIS

<sup>1</sup> Experimental data was at the top of this range and modelling techniques at the lower end

partners. However, the slow corrosion rate ( $\sim 0.01 \mu\text{m}\cdot\text{a}^{-1}$ ) and resulting small amount of volumetric expansion over prolonged timescales, as shown in Table 1, means it is an impractical choice that would need to be heavily accelerated, which may in turn significantly affect grout matrix properties. Magnox therefore provides a compromise between these metals as it possesses a reasonable long-term corrosion rate under ambient temperature conditions, and provides a relatively large volumetric expansion (approximately 580 times greater than that of mild steel over 100 years at 20°C) and can be handled in inactive facilities. Furthermore, any learnings from package expansion should still be applicable to the other metals from a volumetric expansion and package deformation viewpoint. However, following discussions with the PREDIS partners, aluminum is also included as a variant metal due to it being widely applicable across the partner countries as well as potentially not offering the same concerns in terms of the effect on cement phase evolution, which are discussed in the next paragraph.

A point of discussion between the PREDIS partners following the first issue of the technical memorandum was whether the inclusion of Magnox (or aluminium) will alter cement phase formation. It has been shown that a silico-magnesia gel (M-S-H) can be directly synthesised from brucite ( $\text{Mg}(\text{OH})_2$ ) in the presence of silica fume [40], [41]. There is also evidence that C-S-H can be destabilised within a few months in the presence of Mg or M-S-H, with the substitution of Mg for Ca leading to either M-S-H or M-(C)-S-H being formed [42]–[44]. The formation of M-S-H has been linked to both low Ca/Si hydrates [42] and lower pH cement systems [45], both of which are more likely to occur in blended cement systems. However, there is some discrepancy in the literature, with a previous study by Lothenbach et al. finding that synthetic samples containing both calcium and magnesium would form separate C-S-H and M-S-H gels, with little uptake of Mg in the C-S-H or Ca in the M-S-H [46]. Similarly, there is also some evidence that Mg would form hydrotalcite with other Mg phases, instead of substituting into the C-S-H phase [47]. The corrosion product for Magnox or magnesium is brucite [24] which is stable under the high pH conditions found in PC grouts and does not form hydrates,  $\text{Mg}(\text{OH})_2 \cdot x\text{H}_2\text{O}$ . Consequently, it would be expected to remain in that state indefinitely, suggesting the potential for M-S-H or M-(C)-S-H formation is minimal. The work of Cronin and Collier [24] demonstrated that Mg content in the grout depleted rapidly as distance from the corrosion interface increased, supporting the claim that the bulk cement phases within a wasteform will be unaltered. This is supported further by Setiadi et al. [29] who found an interfacial area of  $<100 \mu\text{m}$  extending from the magnesium metal; outside of this intermediary zone the cement was unaltered in terms of phases formed or microstructure compared to control samples.

Setiadi et al. [29] identified the predominant corrosion product formed for aluminium in BFS/OPC grouts to be bayerite with strätlingite,  $\text{Ca}_2\text{Al}[(\text{OH})_6\text{AlSiO}_2(\text{OH})_4] \cdot 5/2\text{H}_2\text{O}$  also present. Bayerite is metastable and ages over the timescale of interest to form gibbsite or nordstrandite. In their study, Setiadi et al. [29] found an interfacial area extending to 2 mm from the edge of the aluminium into the cement phase. Beyond this area showed little change in the phases formed or microstructure compared to the control samples [29]. In their paper, Kinoshita et al. [31] examined the phases present at 21 days curing in OPC and BFS blended cements with varying amounts of aluminium (up to 7 wt %) included. For OPC, it was observed that increasing aluminium decreased portlandite and C-S-H content whilst ettringite, monosulphate and an alumina gel phase increased. The trend was similar for the BFS blended cements, however, the decrease in C-S-H and increase in alumina was less pronounced. Evaluating the literature, it therefore appears that both Magnox and aluminium metal will cause local changes to the cement phases and microstructure, however, the bulk cement would remain essentially unchanged [24], [29], [48].

It is known that Magnox does display an initial higher (acute) corrosion rate than the long-term chronic rate, which is given in this report. However, for the purpose of this study the chronic rate is more applicable to long term storage and degradation issues. The chronic corrosion rate of Magnox shows a temperature dependance [23]–[25]. The following Arrhenius equation can be used to

calculate the corrosion rate (in  $\mu\text{m}\cdot\text{a}^{-1}$ ) for temperatures between 5 and 90 °C [25], which is applicable for corrosion in grout free of chloride content:

$$\text{Rate } (\mu\text{m} \cdot \text{a}^{-1}) = \exp\left[\frac{-13500}{T(K)} + 43.4\right] \times \exp\left[\frac{0.73^2}{2}\right]$$

*Equation 4: Magnox corrosion rate in a grout matrix*

The end term is required to calculate the correct corrosion rate due to the data distribution type. A subsequent report [49] found a chronic corrosion rate of  $0.1 \mu\text{m}\cdot\text{a}^{-1}$ , at 20 °C and  $0.4 \mu\text{m}\cdot\text{a}^{-1}$ , at 30 °C which shows excellent agreement with the corrosion rate equation shown above. When corroding, Magnox will form Brucite ( $\text{Mg}(\text{OH})_2$ ) which has an absolute expansion factor of 1.76 and an effective expansion factor of 2.6-4.1, when accounting for porosity and depending on the degree of constraint imposed by the grout matrix. The corrosion of the Magnox and subsequent formation of brucite leads to a tensile strength development of 0.33 MPa/wt% Magnox corroded [24]. In their report, Cronin and Collier [23] used a loading of 155 kg of Magnox swarf for a 500L drum, which equates to 62 kg for a 200 L drum, assuming a linear correlation. The studies that have examined aluminum corrosion appear to have used a combination of coupons or rods for the metal inclusion in the grout matrix. For the variant degradation mechanism, it is recommended aluminum be treated in the same way as Magnox (or Mg metal). However, the amount of metal included may want to be trialed at smaller scale first to establish whether the large initial hydrogen production will be problematic.

### 3 Reference Package

#### 3.1 Waste package geometry and construction

One reference package has been formulated based on the information available from references [1]–[3]. The data on concrete waste packages was extracted from these three references to create the 54 data entries in the waste package spreadsheet (provided in Table 4). Of these 54 data entries, 26 utilised cylindrical geometry (drums) and 28 used prismatic geometry (boxes). From Table 4 it can be observed that the most common package dimension and geometry combination is the 200-216 L cylindrical packages, therefore this is recommended for the reference package. The most common dimensions are 90 cm in height and 60 cm in diameter.

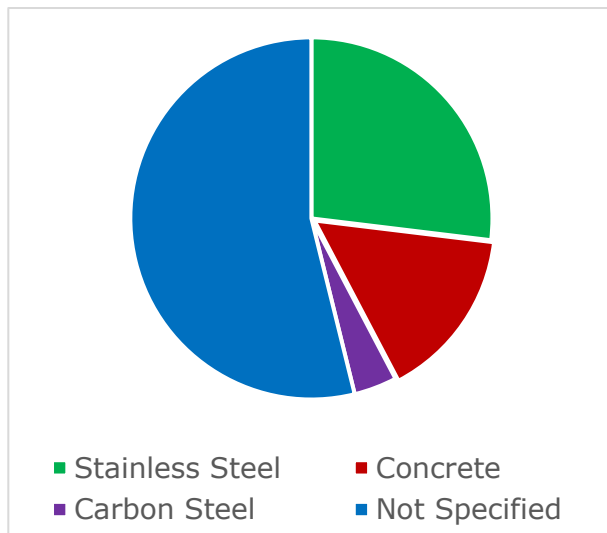


Figure 1: Breakdown of the waste package materials for cylindrical packages

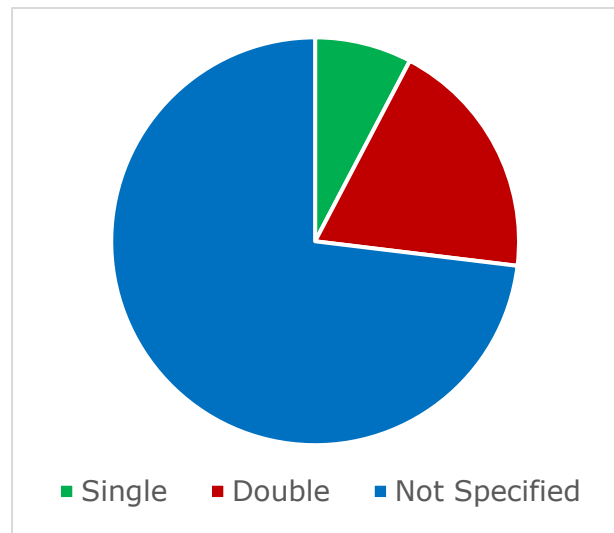


Figure 2: Breakdown of the number of skins associated with cylindrical packages.

Examining the data for key characteristics, where specified, identified stainless steel to be the most common package material, followed by concrete and carbon steel, as shown in Figure 1, which used data from Table 4. No details were provided on the grade of stainless steel used for cylindrical packages in the data based on the SoTA report [1], however, one prismatic package used 304L grade stainless steel and U.K. cylinders use 316L grade stainless steel [50]. For specificity, it is recommended that a 300 grade austenitic stainless steel be adopted for the reference package. For the U.K. cylindrical packages, a skin thickness of 3 mm is used. When examining the data on the package construction type (Figure 2), most data did not provide further breakdown on the number of skins. Where it was provided, double skin construction was the most readily used, which consisted of a 5 cm thick bund of concrete between the steel layers. However, discussion between the PREDIS WP7 partners revealed that the single skin package was the more universal design and so the recommended reference package should be single skinned. Scaling the package skin thickness down from the U.K. specification would result in a 1.2 mm skin for a 200 L package, assuming a linear relationship between volume and skin thickness. To allow partners to tailor the package it is suggested  $1.2 \pm 0.2$  mm be used for the reference package. This calculation appears to be in line with international drum wall thicknesses [51].

A strong trend was found for the grout matrix type used for encapsulation with 92.3% of cylindrical package data entries including pure Portland cement, (PC) formulations and BFS/PC blends in the data. It is recommended that the reference package use a BFS:PC blended system, which is used by three countries, as the reference degradation data is based on this system. For specificity, it is recommended that the U.K. formulation be used as this is well defined and has been studied extensively [17]–[20], [23], [24], [30], [52]. This formulation uses a high replacement (>3:1 wt/wt) BFS:PC mix at a 0.35 - 0.5 water to solids (w/s) ratio [53]. No additives or superplasticisers should be used for this reference package, as no information was provided on this for the SoTA dataset [1] in the majority of cases.

The final specification required for the waste package is the closure system. Most data entries imply a metallic lid is used, with 31 % of the entries also specifying that a concrete or cemented layer is included on top of the solidified waste. Therefore, it is recommended that the reference package utilise a cemented layer between the wasteform and metallic lid. It is recommended that an attempt be made to ensure the cemented wasteform or grout layer are in contact with the metallic lid. It is also recommended that the lid should be constructed from the same material as the package. A

variety of package closure mechanisms were noted, including clamping, screwing and bolting. It is noted that the U.K. entries also included that the lids are vented, which is recommended to be included in the reference package design containing Magnox or Mg (or aluminium as variant) to prevent the pressurisation of the package and the potential generation of high hydrogen concentrations in the ullage of the package.

### 3.2 Other details for reference package

Trends based on waste loading were less clear. For the cylindrical packages it was a 50:50 split between homogeneous and heterogeneous wastefoms, according to the definition prescribed in the WP7.1 SoTA report [1]. Expanding the trending to include the prismatic geometry, showed that 72.2 % of the 54 data entries listed heterogeneous wastefoms whilst 27.8 % of the data was associated with homogenous waste. Therefore, it is recommended that a heterogenous wastefom be used for the reference package, composed of either large discrete metal pieces or smaller pieces that are evenly distributed throughout the grout.

Further to this, little detail was given on the storage conditions of the packages. For specificity, it is recommended that the reference package be stored under the following conditions, which are based on reference [50], [53]:

- Controlled air changes,
- Temperatures between 0 and 20 °C,
- Relative humidity less than 50 %,
- Controlled chloride deposition density on surface of packages<sup>2</sup> (<100 µg<sub>Cl</sub>cm<sup>-2</sup>).

## 4 Conclusions

This document has provided a high-level overview of the different mechanisms reported in the SoTA report as of interest to the end users. This shows that volumetric expansion is a common degradation mechanism consequence, which will lead to cracked cement matrices and could ultimately cause package deformation in the correct circumstances. It is recommended that corrosion from reactive metals will be the largest contributor to this.

This document also provides a summary of the data entries obtained from the SoTA report as to the waste packages currently in use. This was added to reflect U.K. packages, with the overall data set assessed to identify any trends/common characteristics, which were then used to recommend a reference package to be used throughout PREDIS WP7. Table 3 supplies a brief summary of the reference package criteria.

*Table 3: Summary of the reference package details.*

Criteria	Single Skin
Geometry	Cylindrical
Size	200 L (60 cm Ø, 90 cm height)
Construction material	Austenitic Stainless Steel (300 grade, 1.2 ± 0.2 mm thickness)
No. of skins	One
Closing system	Concrete layer between wastefom and lid. Stainless steel (300 grade) lids. Suggested this be vented. Closing system can be screw, clamp or bolted.

<sup>2</sup> This is for solely the chloride content, but it is assumed that the chloride will be in a soluble form e.g. NaCl.

Criteria	Single Skin
Wasteform grout formulation	>3:1 wt/wt BFS: OPC blended mix, 0.35-0.5 w/s, no additives, sand, aggregate or superplasticisers
Waste type	Magnox metal (or Mg). Large discrete pieces or small bits evenly distributed throughout the grout matrix. Recommended use 62kg of Magnox (or Mg).
Storage Environment	0-20 °C, RH < 50%, controlled air change and controlled chloride content (< 100 µg <sub>Cl</sub> ·cm <sup>-2</sup> )

## 5 Optional Variants

It is noted that the reference package specified is quite specific. After conversations following Issue 1 of the technical memorandum it was agreed that aluminium should also be included as a potential reference waste type, which could be implemented in a nearly identical manner to that as Magnox or magnesium.

From discussions with the fellow partners of WP 7, several areas were identified that could be used as potential variants. The first area is package geometry. Out of the 54 data entries collected, 28 used prismatic geometry which is not reflected within the current reference package. It is therefore recommended that if an additional reference package is desired it should be based on a prismatic package.

Examining Table 4, 17 of the 28 entries specify concrete construction, whilst 11 specify steel. Excluding the U.K. entries, the trend becomes more evenly split with 9 entries specifying concrete and 11 specifying steel. It is recommended that if a prismatic package is pursued concrete construction should be used to provide a distinct difference to the cylindrical packages. Only a few entries indicated that steel reinforcement should be used, with most not specifying this. It is therefore recommended that steel reinforcement be used, as it was also specified in the case of some concrete cylindrical packages. Excluding U.K. data entries, the modal value for prismatic package volume was 1500 L, whereas the median value was 1728 L. It is recommended that the 1500 L size be used.

Another area for potential variation is the grout matrix. A BFS:PC blend was supplied for the reference package as it was used in the references used to provide data for the degradation mechanism, such as the metal corrosion rates outlined in this report. A common formulation used throughout the entries was pure PC, and so it is recommended this be used as a potential variant. During a WP 7 workshop it was also discussed that the addition of a larger sized component into the grout formulation, such as a graded limestone, may improve the grout performance due to increasing the resistance to cracks. This could then also be included as an additional variation.

Finally, during the workshop there was some discussion as to a variant for the degradation mechanism. Cellulose was mentioned as a mechanism of interest, where the main consequence relevant to package deformation will likely be gas generation arising from degradation of the cellulosic component in the high alkaline grout matrix environment. As far as these authors are aware, there is limited information on the gas generation data from cellulose encapsulated in a grout matrix, and so obtaining robust baseline data on this may be a worthwhile endeavour to support package evolution and monitoring studies.

## REFERENCES

- [1] S. Uras, "Deliverable 7.1 State of The Art in packaging, storage, and monitoring of cemented wastes 2021-02-23 version 0.9," p. 93.
- [2] "Geological Disposal: Upstream Optioneering - Overview and uses of the 6 cubic metre concrete box (Geological Disposal: Upstream Optioneering Overview and uses of the 6 cubic metre concrete box (18959097)," Nuclear Decommissioning Authority, 2013.
- [3] "Geological Disposal: Waste Package Specification for 500 litre drum waste packages (WPS/300/03)," Nuclear Decommissioning Authority, WPS/300/03, 2013.
- [4] A. Fuller, F. Neall, M. Ferreira, H. Kuosa, M. Hayes, and J. Rasburn, "Review of the Durability of Concretes for ILW Containers and HLW/SF Buffers," *Radioactive Waste Management, RWM/Contr/19/007/2*, 2019.
- [5] B. Šavija and M. Luković, "Carbonation of cement paste: Understanding, challenges, and opportunities," *Constr. Build. Mater.*, vol. 117, pp. 285–301, Aug. 2016, doi: 10.1016/j.conbuildmat.2016.04.138.
- [6] W. Ashraf, "Carbonation of cement-based materials: Challenges and opportunities," *Constr. Build. Mater.*, vol. 120, pp. 558–570, Sep. 2016, doi: 10.1016/j.conbuildmat.2016.05.080.
- [7] Q. Qiu, "A state-of-the-art review on the carbonation process in cementitious materials: Fundamentals and characterization techniques," *Constr. Build. Mater.*, vol. 247, p. 118503, Jun. 2020, doi: 10.1016/j.conbuildmat.2020.118503.
- [8] S. von Greve-Dierfeld *et al.*, "Understanding the carbonation of concrete with supplementary cementitious materials: a critical review by RILEM TC 281-CCC," *Mater. Struct.*, vol. 53, no. 6, p. 136, Oct. 2020, doi: 10.1617/s11527-020-01558-w.
- [9] R. J. Caldwell, N. J. Bowmer, E. J. Butcher, and I. H. Godfrey, "Characterisation of Full-Scale Inactive Cement-Based Intermediate Level Nuclear Wasteforms After One Decade of Storage," in *ICONE12*, 12th International Conference on Nuclear Engineering, Volume 2, Apr. 2004, pp. 681–689. doi: 10.1115/ICONE12-49072.
- [10] Ian Sims and A. Poole, "13 - Alkali–aggregate reactivity," in *Advanced Concrete Technology*, J. Newman and B. S. Choo, Eds. Oxford: Butterworth-Heinemann, 2003, pp. 1–37. doi: 10.1016/B978-075065686-3/50260-3.
- [11] "Seventh meeting of the Contracting Parties to the Joint Convention on the Safety of Spent Fuel Management and on the Safety of Radioactive Waste Management," Kingdom of Belgium, National Report, Oct. 2020.
- [12] F. Vodák, K. Trtík, V. Sopko, O. Kapičková, and P. Demo, "Effect of  $\gamma$ -irradiation on strength of concrete for nuclear-safety structures," *Cem. Concr. Res.*, vol. 35, no. 7, pp. 1447–1451, Jul. 2005, doi: 10.1016/j.cemconres.2004.10.016.
- [13] B. Craeye, G. De Schutter, C. Vuye, and I. Gerardy, "Cement-waste interactions: Hardening self-compacting mortar exposed to gamma radiation," *Prog. Nucl. Energy*, vol. 83, pp. 212–219, Aug. 2015, doi: 10.1016/j.pnucene.2015.03.019.
- [14] P. Soo and L. M. Milian, "The effect of gamma radiation on the strength of Portland cement mortars," *J. Mater. Sci. Lett.*, vol. 20, no. 14, pp. 1345–1348, Jul. 2001, doi: 10.1023/A:1010971122496.
- [15] F. Vodák, V. Vydra, K. Trtík, and O. Kapičková, "Effect of gamma irradiation on properties of hardened cement paste," *Mater. Struct.*, vol. 44, no. 1, pp. 101–107, Jan. 2011, doi: 10.1617/s11527-010-9612-x.
- [16] S. Ishikawa, I. Maruyama, M. Takizawa, J. Etoh, O. Kontani, and S. Sawada, "Hydrogen Production and the Stability of Hardened Cement Paste under Gamma Irradiation," *J. Adv. Concr. Technol.*, vol. 17, no. 12, pp. 673–685, 2019, doi: 10.3151/jact.17.673.
- [17] S. A. Kearney *et al.*, "Effects of plutonium dioxide encapsulation on the physico-chemical development of Portland cement blended grouts," *J. Nucl. Mater.*, vol. 530, p. 151960, Mar. 2020, doi: 10.1016/j.jnucmat.2019.151960.
- [18] J. D. Palmer and G. A. Fairhall, "Properties of cement systems containing intermediate level wastes," *Spec. Double Issue Proc. Symp. E-MRS Fall Meet. 1991*, vol. 22, no. 2, pp. 325–330, Mar. 1992, doi: 10.1016/0008-8846(92)90072-4.
- [19] J. D. Palmer and G. A. Fairhall, "The Radiation Stability of Ground Granulated Blast Furnace Slag/Ordinary Portland Cement Grouts Containing Organic Admixtures," *MRS Online Proc. Libr.*, vol. 294, no. 1, pp. 285–290, Dec. 1992, doi: 10.1557/PROC-294-285.

- [20] M. Angus, M. Hayes, R. Orr, and C. Corkhill, "Behaviour of Alpha Emitters in Cement (16139)," presented at the Waste Management Symposia, 2016.
- [21] C. Paraskevoulakos, D. W. J. Tanner, and T. B. Scott, "Finite element modelling approach to investigate the degradation of intermediate level waste drums induced from interior metallic corrosion," *Eng. Struct.*, vol. 147, pp. 385–397, Sep. 2017, doi: 10.1016/j.engstruct.2017.06.012.
- [22] M. Hayes, S. J. Palethorpe, G. R. Patterson, and G. Woodhouse, "Determination of the Extent of Expansion of Residual Metallic Waste and its Effect on ILW Containers," 2014, p. 4.
- [23] J. Cronin and N. Collier, "Corrosion and expansion of grouted Magnox," *Mineral. Mag.*, vol. 76, no. 8, pp. 2901–2909, Dec. 2012, doi: 10.1180/minmag.2012.076.8.05.
- [24] J. Cronin and N. Collier, "Corrosion & Expansion of Grouted Magnox," Radioactive Waste Management, WT 15 05 10. Accessed: Jun. 28, 2021. [Online]. Available: <https://rwm.nda.gov.uk/publication/corrosion-and-expansion-of-grouted-magnox-november-2011/>
- [25] H. Godfrey and G. Cann, "Effect of Chloride on Magnox Corrosion with Respect to Carbon-14 Release Post Closure," Radioactive Waste Management. [Online]. Available: <https://rwm.nda.gov.uk/publication/effect-of-chloride-on-magnox-corrosion-with-respect-to-carbon-14-release-post-closure/>
- [26] A. Hoch, N. Smart, J. Wilson, and B. Reddy, "A Survey of Reactive Metal Corrosion Data for Use in the SMOGG Gas Generation Model," Serco technologies Consulting Services, ENV-0895, Sep. 2010.
- [27] C. Mendibide, V. Dusquesnes, V. Deydier, X. Bourbon, and D. Crusset, "Corrosion behavior of aluminum alloy 5754 in cement-based matrix-simulating nuclear waste disposal conditions," *Mater. Corros.*, vol. 72, no. 1–2, pp. 383–395, Jan. 2021, doi: 10.1002/maco.202011687.
- [28] K. Fujiwara, J. Tani, M. Hironaga, and Y. Tanaka, "Corrosion behaviour of aluminium under simulated environmental conditions of low-level waste," *Corros. Eng. Sci. Technol.*, vol. 52, no. sup1, pp. 162–165, Apr. 2017, doi: 10.1080/1478422X.2017.1306390.
- [29] A. Setiadi, N. B. Milestone, J. Hill, and M. Hayes, "Corrosion of aluminium and magnesium in BFS composite cements," *Adv. Appl. Ceram.*, vol. 105, no. 4, pp. 191–196, Aug. 2006, doi: 10.1179/174367606X120142.
- [30] H. Godfrey, M. Hayes, D. Anderson, S. Rawlinson, J. Borwick, and J. Clifford, "Corrosion of 1050, 1085, and 5083 grade aluminium in the pore water of a GGBS/CEM I grout up to 777 d," *J. Nucl. Mater.*, vol. 515, pp. 257–266, Mar. 2019, doi: 10.1016/j.jnucmat.2018.12.034.
- [31] H. Kinoshita *et al.*, "Corrosion of aluminium metal in OPC- and CAC-based cement matrices," *Cem. Concr. Res.*, vol. 50, pp. 11–18, Aug. 2013, doi: 10.1016/j.cemconres.2013.03.016.
- [32] L. M. Spasova and M. I. Ojovan, "Characterisation of Al corrosion and its impact on the mechanical performance of composite cement wasteforms by the acoustic emission technique," *J. Nucl. Mater.*, vol. 375, no. 3, pp. 347–358, Apr. 2008, doi: 10.1016/j.jnucmat.2007.11.010.
- [33] M. Jebli, F. Jamin, C. Pelissou, E. Lhopital, and M. S. E. Youssofi, "Characterization of the expansion due to the delayed ettringite formation at the cement paste-aggregate interface," *Constr. Build. Mater.*, vol. 289, p. 122979, Jun. 2021, doi: 10.1016/j.conbuildmat.2021.122979.
- [34] S. Kelham, "12 - Acid, soft water and sulfate attack," in *Advanced Concrete Technology*, J. Newman and B. S. Choo, Eds. Oxford: Butterworth-Heinemann, 2003, pp. 1–12. doi: 10.1016/B978-075065686-3/50259-7.
- [35] R. D. Spence, *Chemistry and Microstructure of Solidified Waste Forms*, First. CRC Press, 1992.
- [36] E. Wieland, G. Kosakowski, B. Lothenbach, and D. A. Kulik, "Geochemical modelling of the effect of waste degradation processes on the long-term performance of waste forms," *Appl. Geochem.*, vol. 115, p. 104539, Apr. 2020, doi: 10.1016/j.apgeochem.2020.104539.
- [37] L. Van Loon, M. A. Glaus, A. Laube, and S. Stallone, "Degradation of Cellulosic Materials Under the Alkaline Conditions of a Cementitious Repository for Low- and Intermediate-Level Radioactive Waste. II. Degradation Kinetics," *J. Environ. Polym. Degrad.*, vol. 7, no. 1, p. 11.
- [38] M. A. Glaus and L. R. Van Loon, "Degradation of Cellulose under Alkaline Conditions: New Insights from a 12 Years Degradation Study," *Environ. Sci. Technol.*, vol. 42, no. 8, pp. 2906–2911, Apr. 2008, doi: 10.1021/es7025517.

- [39] I. Pavasars, J. Hagberg, H. Borén, and B. Allard, "Alkaline Degradation of Cellulose: Mechanisms and Kinetics," *J. Polym. Environ.*, vol. 11, no. 2, pp. 39–47, Apr. 2003, doi: 10.1023/A:1024267704794.
- [40] Z. Zhang, H. Wang, J. L. Provis, F. Bullen, A. Reid, and Y. Zhu, "Quantitative kinetic and structural analysis of geopolymers. Part 1. The activation of metakaolin with sodium hydroxide," *Thermochim. Acta*, vol. 539, pp. 23–33, Jul. 2012, doi: 10.1016/j.tca.2012.03.021.
- [41] S. Walling, "Conversion of magnesium bearing radioactive wastes into cementitious binders," University of Sheffield, 2016.
- [42] C. Roos *et al.*, "Thermodynamic properties of C-S-H, C-A-S-H and M-S-H phases: Results from direct measurements and predictive modelling," *Appl. Geochem.*, vol. 92, pp. 140–156, May 2018, doi: 10.1016/j.apgeochem.2018.03.004.
- [43] E. Bernard, A. Dautères, and B. Lothenbach, "Magnesium and calcium silicate hydrates, Part II: Mg-exchange at the interface 'low-pH' cement and magnesium environment studied in a C-S-H and M-S-H model system," *Appl. Geochem.*, vol. 89, pp. 210–218, Feb. 2018, doi: 10.1016/j.apgeochem.2017.12.006.
- [44] O. P. Shrivastava, S. Komarneni, and E. Breval, "Mg<sup>2+</sup> uptake by synthetic tobermorite and xonotlite," *Cem. Concr. Res.*, vol. 21, no. 1, pp. 83–90, Jan. 1991, doi: 10.1016/0008-8846(91)90034-F.
- [45] A. Dautères *et al.*, "On the physico-chemical evolution of low-pH and CEM I cement pastes interacting with Callovo-Oxfordian pore water under its in situ CO<sub>2</sub> partial pressure," *Cem. Concr. Res.*, vol. 58, pp. 76–88, Apr. 2014, doi: 10.1016/j.cemconres.2014.01.010.
- [46] B. Lothenbach, D. Nied, E. L'Hôpital, G. Achiedo, and A. Dautères, "Magnesium and calcium silicate hydrates," *Cem. Concr. Res.*, vol. 77, pp. 60–68, Nov. 2015, doi: 10.1016/j.cemconres.2015.06.007.
- [47] I. G. Richardson and G. W. Groves, "The incorporation of minor and trace elements into calcium silicate hydrate (C-S-H) gel in hardened cement pastes," *Cem. Concr. Res.*, vol. 23, no. 1, pp. 131–138, Jan. 1993, doi: 10.1016/0008-8846(93)90143-W.
- [48] A. Setiadi, "Corrosion of Metals in Composite Cement," University of Sheffield, 2006.
- [49] A. Hoch and B. Swift, "Modelling the Expansion and Cracking of Grouted Wasteforms Containing Mild Steel or Magnox," Amec Foster Wheeler, Radioactive Waste Management AMEC/002053/001, May 2016.
- [50] "Industry Guidance - Interim Storage - Integrated Approach," Nuclear Decommissioning Authority, Issue 3, Jan. 2017.
- [51] W. Li, X. Liu, M. Li, Y. Huang, and S. Fang, "Multilayer Shielding Design for Intermediate Radioactive Waste Storage Drums: A Comparative Study between FLUKA and QAD-CGA," *Sci. Technol. Nucl. Install.*, vol. 2019, p. 8186798, Apr. 2019, doi: 10.1155/2019/8186798.
- [52] D. P. Prentice, B. Walkley, S. A. Bernal, M. Bankhead, M. Hayes, and J. L. Provis, "Thermodynamic modelling of BFS-PC cements under temperature conditions relevant to the geological disposal of nuclear wastes," *Cem. Concr. Res.*, vol. 119, pp. 21–35, May 2019, doi: 10.1016/j.cemconres.2019.02.005.
- [53] "Geological Disposal - Waste Package Evolution Status Report," Radioactive Waste Management, Issue 2 DSSC/451/01, Dec. 2016.

Table 4: Summary of the spreadsheet containing the waste package information.

Material	Steel Reinforcement	Steel type	Matrix	Matrix Additions	Package Shape	Skins	Package Volume (Litres)	Closure System	Pre-Treatment	Conditioning	Waste Classification	Main Element	Waste Type
Concrete	Y	N/A	BFS:PC Blends		Cylindrical		1000	Concrete lid cast after waste solidification		Homogeneous	ILW		
Steel	NA	Not Specified	Bitumen		Cylindrical		60 - 216	sealed lid		Homogeneous			
Steel	NA	Stainless	OPC		Cylindrical		200	upper lid with a ring plus screw for 200, and upper lid for metallic	In-Drum mixed	Homogeneous	LLW		Sludge
Steel	NA	Stainless	OPC		Prismatic		1500	upper lid with a ring plus screw for 200, and upper lid for metallic	In-Drum mixed	Homogeneous	LLW		Sludge
Steel	NA	Not Specified	Sulfate Resistant Portland cement	Zeolites (for sorption)	Cylindrical		200	Lid, screwed or clamping ring		Homogeneous	LLW		Sludge

Material	Steel Reinforcement	Steel type	Matrix	Matrix Additions	Package Shape	Skins	Package Volume (Litres)	Closure System	Pre-Treatment	Conditioning	Waste Classification	Main Element	Waste Type
Steel	NA	Not Specified	Sulfate Resistant Portland cement	Zeolites (for sorption)	Cylindrical		200	Lid, screwed or clamping ring		Homogeneous	LLW		Concentrates
Steel	NA	Not Specified	OPC		Cylindrical		200	Locking clips	Dewatered; In-Drum mixed	Homogeneous	ILW		
Steel	NA	Carbon	OPC		Cylindrical		200	Double lid	Thermal	Homogeneous	LLW		
Steel	NA	Not Specified	Sulfate Resistant Portland cement	Zeolites (for sorption)	Cylindrical		200	Lid, screwed or clamping ring		Homogeneous	LLW		Resins
Steel	NA	Not Specified	OPC		Cylindrical	Double; 5cm Concrete	200	cemented on top, then closed with steel lid	Compression	Homogeneous			Mixed waste
Steel	NA	Stainless	OPC		Cylindrical		2196	bolted lid, metallic gasket	Alkalinization	Homogeneous	ILW		

Material	Steel Reinforcement	Steel type	Matrix	Matrix Additions	Package Shape	Skins	Package Volume (Litres)	Closure System	Pre-Treatment	Conditioning	Waste Classification	Main Element	Waste Type
Steel	NA	Not Specified	OPC		Cylindrical	Double; 5cm Concrete	200	Cemented on top. Then closed by lid	Compaction	Homogeneous	LLW		Mixed waste
Concrete	Y	N/A	BFS:PC Blends		Cylindrical		1000	Concrete lid cast after waste solidification	Evaporation; Cs Separation	Homogeneous	LLW		
Steel	NA	Not Specified	OPC		Cylindrical		216	sealed lid with screw	Polymer solidification	Homogeneous	LLW		
Steel	NA	Stainless	OPC		Prismatic		1000	-		Homogeneous	-		
Steel	NA	Stainless	OPC		Prismatic	Double, 5cm mortar	1500	upper lid		Heterogeneous	?		
Steel	NA	Stainless	OPC		Prismatic	Double, 5cm mortar	1500	upper lid		Heterogeneous	LLW mainly but some ILW		Rubble
Concrete	Unknown	N/A	Lightweight Cement		Prismatic		9600	Concrete lid		Heterogeneous	LLW		Rubble
Concrete	Unknown	N/A	OPC		Prismatic		1200	Concrete lid	Polymer solidification	Heterogeneous	LLW		
Steel	NA	Not Specified	OPC		Cylindrical		216	sealed lid with screw	Sorting	Heterogeneous	LLW		
Steel	NA	Not Specified	OPC		Cylindrical	Double; 5cm Concrete	200	Cemented on top. Then closed by lid	Compacting	Heterogeneous	LLW		Mixed waste

Material	Steel Reinforcement	Steel type	Matrix	Matrix Additions	Package Shape	Skins	Package Volume (Litres)	Closure System	Pre-Treatment	Conditioning	Waste Classification	Main Element	Waste Type
Steel	NA	Not Specified	OPC		Cylindrical		216	sealed lid	Sorting; Fragmentation	Heterogeneous	LLW		
Steel	NA	Not Specified	Sulfate Resistant Portland cement; Lightweight Cement		Cylindrical		200	screwed lid or clamping ring		Heterogeneous	LLW	Al, Cu, stainless steel	Scrap; Smaller metal scrap
Concrete	Unknown	N/A	Sulfate Resistant Portland cement; Lightweight Cement		Prismatic		4500	concrete lid		Heterogeneous	LLW	Al, Cu, stainless steel	Scrap; Smaller metal scrap
Concrete	Unknown	N/A	Sulfate Resistant Portland cement; Lightweight Cement		Prismatic		6240	concrete lid		Heterogeneous	LLW	Al, Cu, stainless steel	Scrap; Smaller metal scrap
Concrete	Unknown	N/A	Sulfate Resistant Portland cement; Lightweight Cement		Prismatic		9600	concrete lid		Heterogeneous	LLW	Al, Cu, stainless steel	Scrap; Smaller metal scrap
Steel	NA	Stainless	OPC		Prismatic		5156	bolted lid, metallic gasket	Compaction	Heterogeneous	LLW		
Concrete	Unknown	N/A	OPC		Prismatic		1728	clean layer on top of steel container or concrete lid for concrete container		Heterogeneous	LLW		

Material	Steel Reinforcement	Steel type	Matrix	Matrix Additions	Package Shape	Skins	Package Volume (Litres)	Closure System	Pre-Treatment	Conditioning	Waste Classification	Main Element	Waste Type
Steel	NA	Not Specified	OPC		Prismatic		1728	clean layer on top of steel container or concrete lid for concrete container		Heterogeneous	LLW		
Concrete	Unknown	N/A	Lightweight Cement		Prismatic		9600	Concrete lid		Heterogeneous	LLW	Steel	Metal scrap pellets
Concrete	Unknown	N/A	Lightweight Cement		Prismatic		6240	Concrete lid		Heterogeneous	LLW	Steel	Large components
Steel	NA	Stainless	OPC		Prismatic	Double, 5cm mortar	1500	upper lid		Heterogeneous	LLW		Sources
Steel	NA	Stainless	OPC		Cylindrical	Double, 5cm mortar	200	upper lid		Heterogeneous	LLW		Sources
Steel	NA	Stainless	OPC		Prismatic	Double, 5cm mortar	1500	upper lid		Heterogeneous	LLW		Cartridge filters
Steel	NA	Stainless	OPC		Cylindrical	Double, 5cm mortar	200	upper lid		Heterogeneous	LLW		Cartridge filters
Concrete	Y	N/A	OPC		Cylindrical		3859	single concrete lid		Heterogeneous	LLW		
Steel	NA	Not Specified	BFS:PC Blends		Cylindrical		400	Seam folding	Incineration; Compaction	Heterogeneous	LLW		
Steel	NA	Not Specified	BFS:PC Blends		Cylindrical		400	Seam folding	Incineration; Compaction	Heterogeneous	ILW		
Concrete	Y	N/A			Cylindrical		665			Heterogeneous	LLW		

Material	Steel Reinforcement	Steel type	Matrix	Matrix Additions	Package Shape	Skins	Package Volume (Litres)	Closure System	Pre-Treatment	Conditioning	Waste Classification	Main Element	Waste Type
Steel	NA	Not Specified	OPC		Prismatic		1728	protective clean layer of concrete		Heterogeneous	LLW		
Concrete	Unknown	N/A	Bitumen		Prismatic		1728	concrete lid		Heterogeneous	LLW		
Steel	NA	Stainless	OPC; Altri non specification		Prismatic		1000	-		Heterogeneous	-		
Concrete	Y	N/A	FA:RHPC <sup>3</sup>		Prismatic		6000	Concrete lid		Heterogeneous	ILW		Activated and Contaminated Metals
Concrete	Y	N/A	FA:RHPC		Prismatic		6000	Concrete lid		Heterogeneous	ILW		Activated and contaminated other materials e.g. concrete
Concrete	Y	N/A	FA:RHPC		Prismatic		6000	Concrete lid		Heterogeneous	ILW		Graphite ILW
Concrete	Y	N/A	FA:RHPC		Prismatic		6000	Concrete lid		Heterogeneous	ILW		Mixed waste
Concrete	Y	N/A	Fine iron oxide: RHPC		Prismatic		6000	Concrete lid		Heterogeneous	ILW		Activated and Contaminated Metals

<sup>3</sup> FA:RHPC is a blend of fly ash (FA, formerly pulverised fly ash) and rapid hardening Portland cement

Material	Steel Reinforcement	Steel type	Matrix	Matrix Additions	Package Shape	Skins	Package Volume (Litres)	Closure System	Pre-Treatment	Conditioning	Waste Classification	Main Element	Waste Type
Concrete	Y	N/A	Fine iron oxide: RHPC		Prismatic		6000	Concrete lid		Heterogeneous	ILW		Activated and contaminated other materials e.g. concrete
Concrete	Y	N/A	Fine iron oxide: RHPC		Prismatic		6000	Concrete lid		Heterogeneous	ILW		Graphite ILW
Concrete	Y	N/A	Fine iron oxide: RHPC		Prismatic		6000	Concrete lid		Heterogeneous	ILW		Mixed waste
Steel	NA	Stainless	BFS:PC Blends		Cylindrical		500			Heterogeneous	ILW		
Steel	NA	Stainless	BFS:PC Blends		Prismatic	Double Skinned	3000			Heterogeneous	ILW		
Steel	N/A	Stainless	BFS:PC Blends		Cylindrical	Single skin	560	Concrete lid; steel flange; vented	Controlled	Heterogeneous	ILW		Reactive Metal
Steel	N/A	Stainless	BFS:PC Blends		Cylindrical	Single Skin	560	Concrete lid; steel flange; vented	Controlled	Heterogeneous	ILW	Uranium	Reactive Metal